applied sciences

MDPI

Article

Parameter Calibration and Optimization of a Discrete Element Model of Plug Seedling Pots Based on a Collision Impact Force

Ji Cui, Xuying Li *, Fandi Zeng, Hongbin Bai and Yongzhi Zhang

College of Mechanical and Electrical Engineering, Inner Mongolia Agricultural University, Hohhot 010018, China
* Correspondence: lixuy2000@imau.edu.cn

Abstract: To improve the accuracy of simulation parameters used in discrete element simulation tests for the transplanting operation of the transplanting machine and to facilitate further optimization of crucial components of the transplanting machine, in this paper, the discrete element model of 50-hole plug seedling pots was calibrated and optimized based on the collision impact force between the plug seedling pot and the steel plate measured by a flexible film network tactile pressure sensor. Basic tests determined the contact parameters of the pot, and the initial parameters were screened for significance using the Plackett–Burman test. The pot-steel static friction coefficient, the pot-pot collision restitution coefficient, and the bond radius significantly affected the simulated collision impact force between the pot and the steel plate. According to the relative error value of the impact force between the pot and the steel plate as the evaluation index, the steepest climbing test was carried out on three significant parameters to optimize their value range. Based on the Box–Behnken test, a second-order regression model of the impact force and significant parameters regulating the interaction between the pot and the steel plate was established, where the target impact force between the pot and the steel plate was 11.78 N. The optimal parameter combination is obtained by optimizing the significance parameters: the static friction coefficient between the pot and steel is 0.790, the collision restitution coefficient between the pot and the pot is 0.325, and the bond radius is 1.542 mm. The test results show that the relative error between the actual and simulation tests is only 0.084%. The calibrated parameters of the discrete element model of plug seedling pots are accurate and reliable. The research results presented here can provide a reference for the subsequent transplanting operation simulation of the transplanter.

Keywords: plug seedling pots; collision impact; discrete element; parameter calibration

Citation: Cui, J.; Li, X.; Zeng, F.; Bai, H.; Zhang, Y. Parameter Calibration and Optimization of a Discrete Element Model of Plug Seedling Pots Based on a Collision Impact Force. *Appl. Sci.* **2023**, *13*, 6278. https://doi.org/10.3390/app13106278

Academic Editor: Roberto Romaniello

Received: 27 January 2023
Revised: 24 April 2023
Accepted: 19 May 2023
Published: 20 May 2023

1. Introduction

As one of the critical oil crops in China, the demand for sunflower oil is gradually increasing with the continuous improvement of the living standard of people [1]. Seedling transplanting of oil sunflowers can shorten the growth period of crops and significantly increase the yield per unit area of crops, which is higher than direct seeding and has high economic benefits [2]. Inner Mongolia is one of the leading oil sunflower planting areas in China, and the use of transplanters for mechanized planting and transplanting can significantly improve production efficiency [3].

To improve the performance of transplanters, increasingly higher requirements are placed on the working parts that are in direct contact with the pot of the plug seedling [4–6]. Ma et al. studied the physical properties of the pot by compression tests. They obtained the factors affecting the size of the pot under crushing, which provided an essential reference basis for the subsequent design of the end-effector and optimization of the structural parameters [7]. Zeng et al. conducted trials using high-speed photography applied to a hanging cup transplanting tester to determine the optimal combination of casting parameters affecting plug seedlings [8]. Hu et al. optimized the top pinch-pull seedling extraction device to address the low success rate of seedling extraction and high rate of pot breakage and determined the optimal working parameter combination through experimental analysis [9]. Previous studies have carefully investigated various aspects of the pot's physical properties, the seedlings' movement pattern, and the working parts in contact with them. However, the interaction of the working parts in contact with microscopic particles is less studied.

With the rapid development of computer technology, the discrete element method (DEM)-based approach for the optimal design of critical components of agricultural machinery has become one of the crucial tools of research in this area [10–13]. The discrete element method can be used to simulate the particle materials and to study the interactions between the materials to analyze the forces and movements of the plug seedling particles during transplanting [14–16]. The credibility of discrete element simulations depends mainly on the selection of its contact model and the setting of simulation parameters, so it is vital to study the contact model and parameter calibration [17]. In the simulation analysis using discrete element-related software simulation, it is necessary to calibrate the parameters of the physical and mechanical characteristics of the pot of plug seedlings, the contact between the pot and the transplanter, and other parameters to provide preparatory work for the application of the discrete element method for research related to plug seedling transplanting. Scholars have performed much research on agricultural materials using the discrete element method. Wang et al. [18] calibrated the contact parameters between corn seed particle models by combining the simulation of the corn seed accumulation angle with the actual test, providing a theoretical basis for the structural design and parameter optimization of the metering device. Zhang et al. [19] calibrated rice seeds by cylinder lifting and slide stacking tests using the coefficient of variation of the rest angle of the simulation test as an index and studied the effect of different filled ball radii of the rice seed model on the kinetic response characteristics between particles. Zhang et al. [20] measured the contact parameters of soybean seeds and seeders and calibrated the discrete element based on the natural angle of the repose test, providing a basis for the parameter setting of the discrete element numerical simulation of the soybean seeding test. Shi et al. [21] established a flexible model of flax stalk verified by shear test and stacking angle test. Previous studies have primarily calibrated the parameters of the discrete element model of various agricultural materials using the stacking angle and the angle of repose. However, there are few reports on calibrating the parameters of the discrete element model of oil sunflower plug seedling pots. At present, many scholars have measured individual parameters to set the initial value of the discrete element simulation of the pot [22–24]. Few comprehensive physical tests are used to measure the parameters of the pot, and the discrete element simulation parameters of the pot are calibrated based on the physical test parameters.

In this paper, based on the existing research, a discrete element model of 50-hole plug seedling pots was calibrated by applying the experimental method of collision impact force between the pot and the steel plate measured by a flexible film network tactile pressure sensor. To obtain more accurate discrete element simulation input parameters, first, the contact parameters are measured, the pot-free fall impact test is carried out, and the pot drop impact model is established with the help of EDEM software based on relevant research. Through the Plackett–Burman test, the steepest climbing test, and the Box–Behnken test, combined with the test optimization design method, the discrete element simulation parameters of the pot were calibrated and optimized. Finally, the simulation parameters of the discrete element model of the 50-hole oil sunflower plug seedling pots were verified and determined to promote the application of the discrete element method in the optimal design of the transplanter, thereby improving its performance.

2. Materials and Methods

2.1. Test Materials and the Morphological Parameter Measurements

The experiment utilized the 50-hole oil sunflower variety T562, cultivated by Inner Mongolia Heyuan Agricultural Science and Technology Company Limited. The pot of the plug seedling was made of peat, vermiculite, and perlite according to the matrix formula, with a volume ratio of 3:1:1. The seedling age was 30 days, with a moisture content of approximately 52%. Healthy seedlings of oil sunflower with good growth, a well-developed root system, an excellent enveloping degree, no symptoms of disease or insect pests, and no prominent lodging were selected, as shown in Figure 1.

(a)

(b)

Figure 1. 50-hole oil sunflower plug seedlings (**a**) Front view; (**b**) Top view.

Each plant's height and spreading were measured using a scale for each of the 50-hole oil sunflower plug seedlings selected from 5 whole plates. Vernier calipers measured the corresponding stem diameter, and an electronic scale weighed the single plant mass of each tray of anemone seedlings. The changes in morphological characteristics were plotted as shown in Figure 2. From the a-c diagram, it can be found that the height of oil sunflower seedlings in the 50-hole is 132~172 mm, with good growth. The range of leaf spread size of oil sunflower seedlings is 107~157 mm, and the range of stem diameter is 1.4~3.5 mm, which is relatively robust. From Figure 2d, it can be seen that the range of single plant mass of the 50-hole oil sunflower seedlings is 13~23 g, and the overall quality is similar.

The morphological distribution table of oil sunflowers is shown in Table 1. The coefficients of variation were less than 15%, indicating that the data were standard. By calculating the height and leaf spread of 50-hole plug seedlings, it can be seen that the two fluctuate greatly, which may be caused by the uneven substrate during the filling process of plug seedlings or the variability of artificial seedlings, resulting in their nonuniform nutrients and the marginal effect of plants. The amount of substrate in the roots of plug seedlings and the loss of substrate by watering may also affect the height of plug seedlings. The calculated statistics of the mass of a 50-hole plug seedling per plant indicate that the weight of the same plug seedling varies little. Although there were variations among plants, the overall growth level was good, so it was determined that the selected plug seedlings were healthy and met the planting and testing requirements.

Table 1. Distribution table of morphological characteristic parameters of 50-hole oil sunflower plug seedling.

Morphological Character	Average Value	Variance	Standard Deviation	Coefficient of Variation
Plant height/mm	151.14	88.00041	9.286571	0.061444
Leaf spread/mm	126.12	130.9649	11.32897	0.089827
Stem diameter/mm	2.6332	0.134022	0.362411	0.137631
Single plant mass/g	19.7564	6.324983	2.489675	0.126019

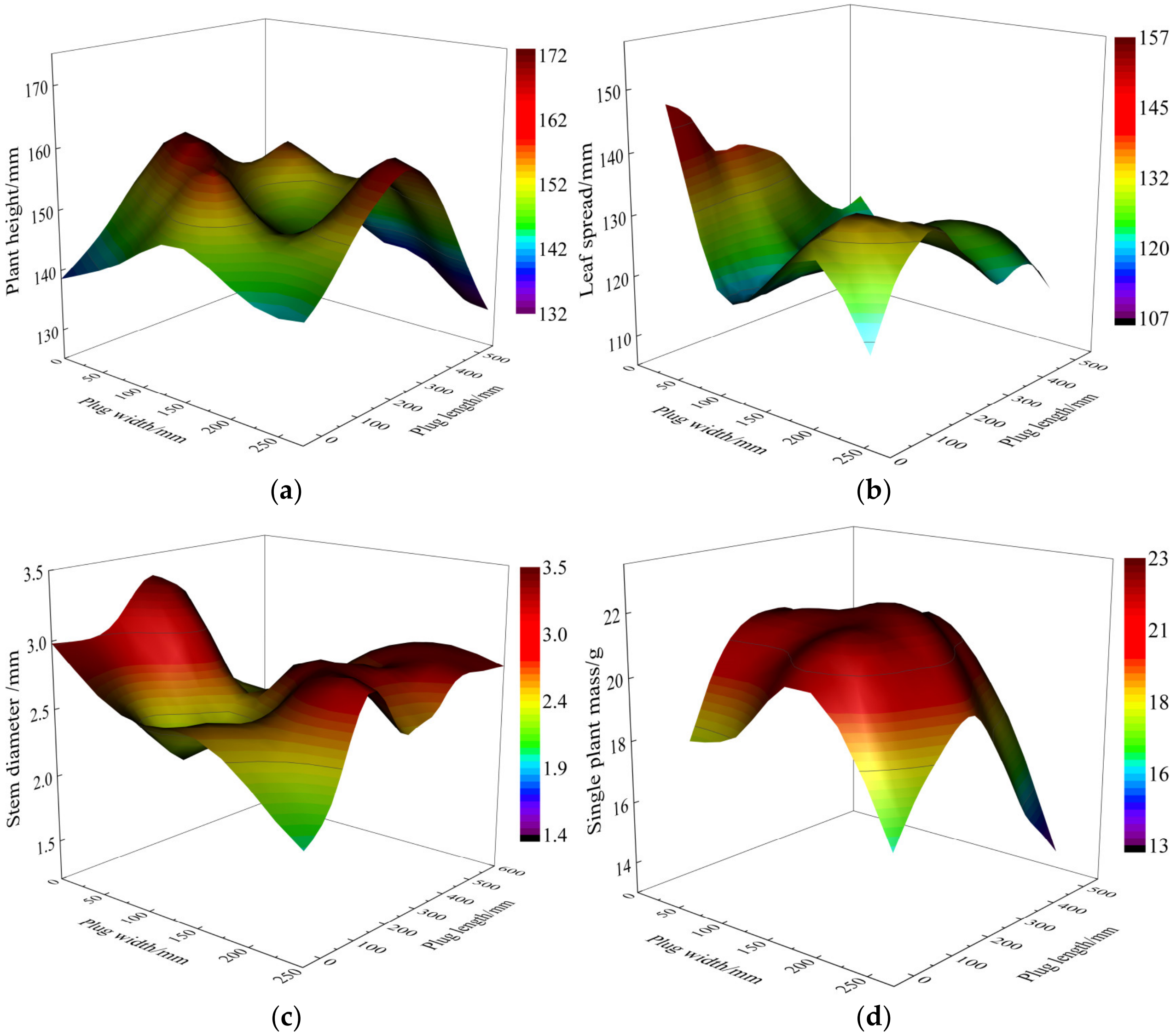

Figure 2. Variation of morphological characteristics of oil sunflower of 50-hole oil sunflower plug seedling (**a**) Plant height; (**b**) Leaf spread; (**c**) Stem diameter; (**d**) Single plant mass.

2.2. Determination of Contact Parameters

The contact parameters to be measured include the collision restitution coefficient and static friction coefficient between the pot and the pot and between the pot and the main of the transplanter. The measured parameter values provide data support for the following discrete element simulation input parameters.

The contact parameter physical test material is an oil sunflower 50-hole plug seedling pot, and its density is 290.2 kg/m^3 after measurement. In agricultural equipment, the primary material of the transplanter planter is Q235 steel, with a Poisson's ratio of 0.28, a density of 7850 kg/m^3, and a shear modulus of 8.2×10^4 MPa [25,26].

2.2.1. Determination of the Collision Restitution Coefficient

A Q235 steel plate and oil sunflower 50-hole seedling pot were selected for the test. The free-falling drop test was carried out on the plug seedling pot, as shown in Figure 3 below.

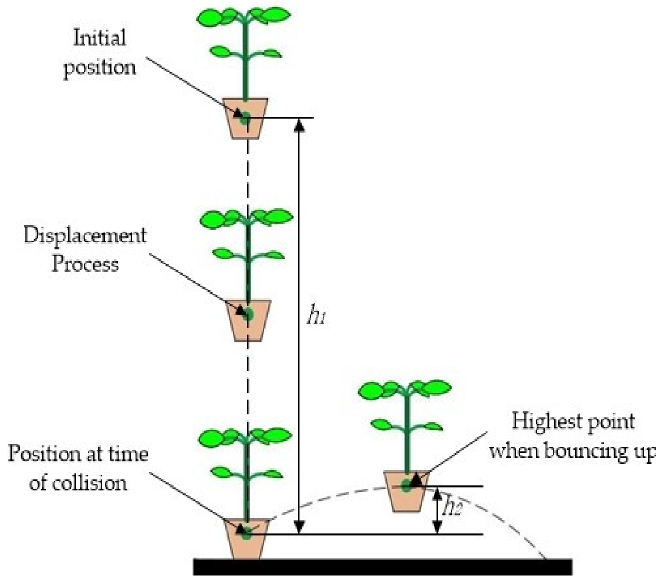

Figure 3. Principle schematic of restitution coefficient measuring device.

The middle part of the pot of the oil sunflower 50-hole plug seedling was marked with pigmented dots to facilitate subsequent capture of the movement trajectory. The stalks of the seedlings were clamped with a gripper and released from a height of 350 mm to free fall and collide with a steel plate (or potting substrate block) located directly below the base. A Pco.dimax S4 high-speed camera was placed at a suitable distance and height in front of the iron stand to capture the whole process. After the test was completed, the motion of the pot during each collision was tracked by TEME software to determine its trajectory characteristics. In this process, to facilitate the relationship image processing of displacement using TEMA, it is necessary to first establish a two-dimensional coordinate system on the test bench and measure the distance from the high-speed camera to the coordinate system and the seedling pot. The distance between the high-speed camera lens and the test surface is 2000 mm, the horizontal distance is set to 400 mm, and the vertical distance is set to 700 mm in TEMA. The distance between the high-speed camera lens and the test surface is 2000 mm.

TEMA software was used to analyze the motion process of the filmed pot, plot the obtained displacement–time curves of the pot-pot and the pot-steel plate collision motion, and then determine the collision restitution coefficient, as shown in Figure 4.

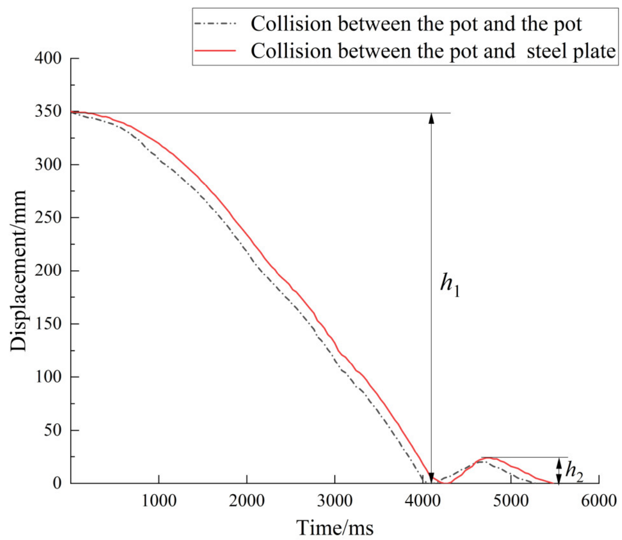

Figure 4. Displacement–time curve of the collision between pot and measured object.

The collision recovery factor is defined as the ratio of the relative velocities to the contact points before and after the collision [27].

Before the collision, the seedling pot made a free fall motion, ignoring the influence of air resistance, according to the kinematics formula:

$$v_{\mathrm{on}} = gt_1 \tag{1}$$

$$h_1 = \frac{1}{2}g{t_1}^2 \tag{2}$$

where v_{on} is the instantaneous velocity of the seedling pot before the collision, m/s; g is the acceleration due to gravity, m/s^2; t_1 is the time of the first free fall, s; and h_1 is the height of the free fall, mm.

After the collision, when the seedling pot reaches the highest point, the speed will drop to zero according to the motion formula:

$$v = v_0 + gt^2 \tag{3}$$

$$h2 = v_0 t_2 + \frac{1}{2}g{t_2}^2 \tag{4}$$

where v is the speed at which the rebound reaches the highest point after the collision, m/s; v_0 is the instantaneous velocity of the oil sunflower seedling pot after the collision, m/s; t_2 is the time when the rebound reaches the highest point after the collision, s; and h_2 is the height of the highest point after the collision, mm.

From the definition of the collision restitution coefficient, the collision restitution coefficient is

$$\mathrm{e} = \frac{v_0}{v_{\mathrm{on}}} = \sqrt{\frac{h_2}{h_1}} \tag{5}$$

After several tests, the range of the collision restitution coefficient between the pot and the pot is 0.29~0.36, and the range of the collision restitution coefficient between the pot and steel is 0.18~0.27.

2.2.2. Determination of the Static Friction Coefficient

The static friction coefficient between the pot and the pot and between the pot and steel was measured using a CNY-1 inclinometer [28,29]. The test surface was selected from the stemless part of the pot of a 50-hole plug seedling pot of oil sunflower, the base of the inclinometer was placed horizontally, and the digital inclinometer was placed above the horizontal plane of the inclinometer before the test. The test plane of the inclinometer was adjusted so that the digital inclinometer indicated 0°.

The static friction coefficient of the pot and the pot were measured, as shown in Figure 5. The pot substrate block is placed inside the ring knife, and the lower surface of the ring knife is glued to the inclinometer test plane using pressure-sensitive adhesive tape to prevent relative sliding. Then, the pot is placed on the measuring plane of the pot substrate block along the length of the inclinometer test plane. The inclinometer test plane is slowly turned counterclockwise until the pot is observed to slide on the measurement plane. Then, turning is stopped, and the digital display inclinometer is recorded at this time.

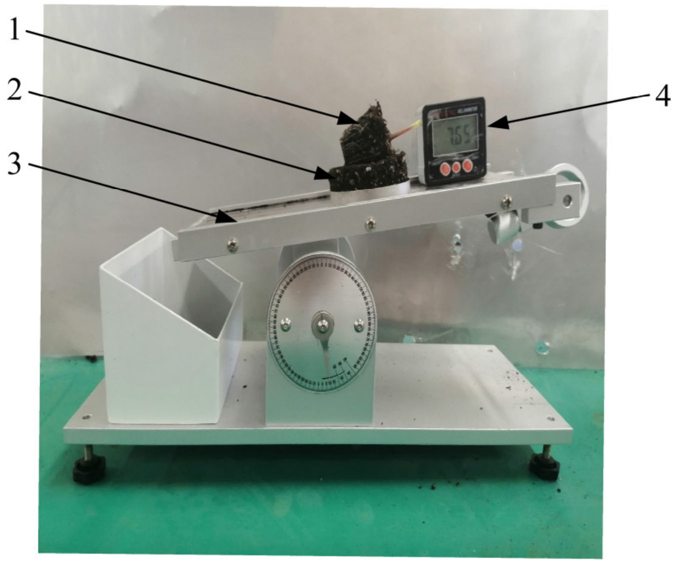

Figure 5. Tests of friction coefficient between the pot and the pot. 1. The Pot 2. Pot substrate block 3. CNY-1 inclined plane tester test plane 4. Digital display inclinometer.

The static friction coefficient between the pot and the pot plane is calculated by Equation (6). Only the pot substrate block ring knife was replaced with the steel plate when measuring the static friction coefficient between the pot and steel. Each group of measurements was carried out five times, and the average was taken as the final value to obtain the range of static friction coefficient between the pot and the pot as 0.86~0.92 and the range of static friction coefficient between the pot and steel as 0.73~0.85.

$$\mu 1 = \tan \varphi 1 \tag{6}$$

where μ_1 is the static friction coefficient relative to φ_1; φ_1 is the indication of the digital display inclinometer when the pot started to slide on the measuring plane (°).

2.3. Drop Impact Force Test

During the whole transplanting process, the interaction of contact and collision mainly occurs between the plug seedling and the transplanter planter, so the Q235 steel plate is selected as the material for the collision test, and the subsequent relevant calibration is carried out.

The drop impact test device is shown in Figure 6, where the whole 50-hole plug seedling pot is dropped, and the 50-hole plug seedling pot with the leafy stalks removed (the 20 mm stalks above the pot are retained to facilitate the clamping of the seedling by the seedling clamp) is tested for free drop impact using an iron stand. The stalks were clamped with the chuck and then released from the same 350 mm height for free drop and collided with a steel plate located on the base directly below, which was covered with a 5250 flexible film network of tactile pressure sensors and connected to the I-Scan System data processing system on a computer via a USB terminal. Before the test begins, the iron stand is adjusted so that the pot falls as close to the center of the pressure sensor as possible and lies flat on the surface of the collision material. The sensor is calibrated and zeroed to ensure the accuracy of the test data.

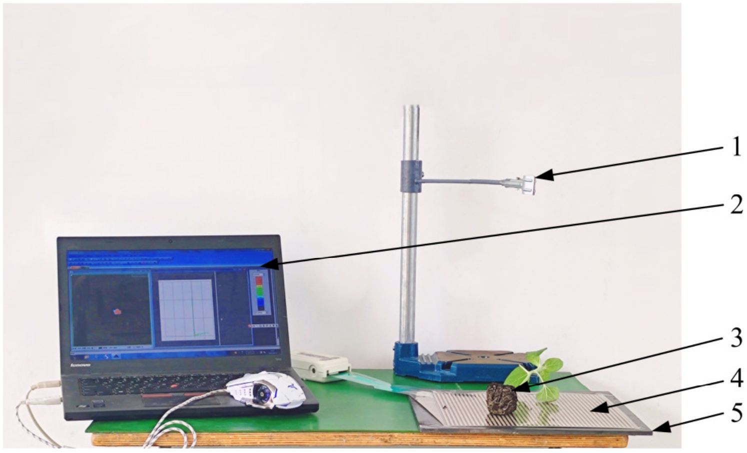

Figure 6. Drop crash test device. 1. Seedling clamp; 2. I-Scan System data processing system; 3. cavity seedling bowl; 4. 5250 flexible film network tactile pressure sensor; 5. steel plate.

In this study, the pressure distribution measurement system of Tekscan Company in the United States is mainly composed of a flexible film network tactile pressure sensor, USB terminal, and I-Scan System data processing system. It can carry out static and dynamic measurements of contact stress and display the contact stress distribution in real-time through intuitive and vivid two-dimensional and three-dimensional images [30,31]. The 5250 model flexible film network tactile pressure sensor has a sensor size of 245.9 × 245.9 mm, a sensor spatial resolution of 3.2/cm^2, a pressure measurement range of 0~0.179 MPa, and a scanning frequency of 0~100 Hz.

After the drop test, the data and images are processed. The two-dimensional touchdown area and pressure distribution nephogram of the whole 50-hole plug seedling pot (and the pot with the stem part removed) generated on the I-Scan System data processing system on the computer during the collision with the steel plate are shown in Figure 7. Each group of tests was repeated five times, and the average value was taken as the final value. Finally, the impact force between the whole 50-hole plug seedling pot and the steel plate was 11.78 N, and the impact force between the 50-hole plug seedling pot and the steel plate was 10.56 N without the leafy stem. The impact force error analysis of the two is shown in Table 2. The difference in impact force between the two is less than 15%. To simplify the model of the hole seedling and improve the calculation efficiency, the 50-hole plug seedling pot with the leafy stem removed is used as the research object instead of the whole 50-hole plug seedling pot.

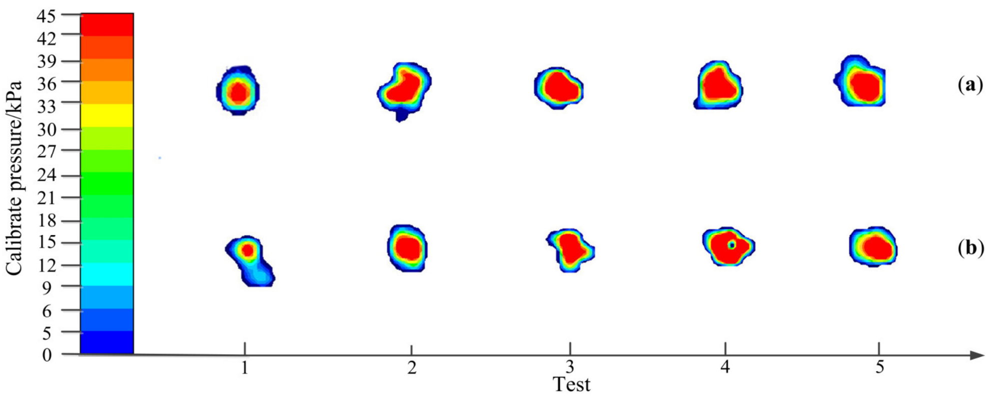

Figure 7. The two-dimensional touchdown area and pressure distribution nephogram. (**a**) Drop impact force of the whole plug seedling pot; (**b**) Drop impact force of the pot.

Table 2. The Impact force error analysis table.

Parameter	1	2	3	4	5	Average Value
Falling impact force of the whole plant/N	10.92	11.96	11.82	12.58	11.62	11.78
Drop impact force of the pot/N	9.87	10.78	10.65	11.01	10.51	10.56
Relative error/%	10.6	9.9	9.9	12.5	9.6	10.40

3. Establishment of the Discrete Element Model of Pot Drop Collision

The pot is in the shape of a square pyramid. To establish the simulation model of an oil sunflower 50-hole plug seedling pot and improve the simulation accuracy, 50 pots of 50-hole plug seedling pots were randomly selected in this paper, and the upper edge length a, the lower bottom edge length b, and the platform height h were measured using a Vernier caliper. The average upper and bottom edge length of 50 mm, the lower bottom edge length of 22 mm, and the platform height of 50 mm were obtained. Therefore, a four-pronged model of the pot was built using Pro/E software and imported into EDEM. The Hertz–Mindlin With Bonding model has normal and tangential contact forces, a material model formed by bonding multiple small particles, and has flexible characteristics. Bond bonds are formed on the contact surface of each particle after bonding. When the external force exceeds the critical value, the material will be squeezed and collide, and the bonding bond will be broken. Therefore, the Hertz–Mindlin with bonding model is used as the bonding model of particles. Based on the Hertz–Mindlin with bonding model, the discrete element model of the bowl is obtained by particle replacement.

After generating the replacement particle plant at 350 mm below the plane of the steel plate and setting the relevant parameters of the steel plate, the pot underwent free fall, impacting the steel plate and completing the simulation, where the EDEM postprocessing function was used to analyze the impact of the pot falling on the steel plate. The establishment process of the discrete element model of pot drop collision is shown in Figure 8.

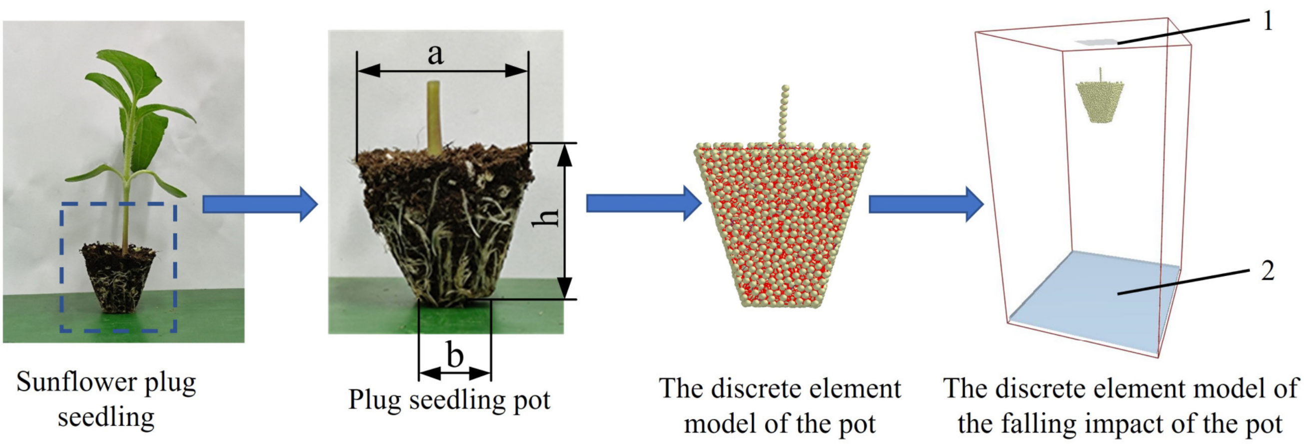

Figure 8. The establishment process of discrete element model of pot drop collision. a. The upper edge length; b. The lower bottom edge length; h. The pot height; 1. Particle factory; 2. Steel plate.

4. Calibration Test of Plug Seedling Pot Simulation Model

4.1. Plackett–Burman Test

This study is based on the measured values of physical tests and refers to the relevant literature [32–34]. It is determined that the Poisson's ratio of the pot is 0.38, the shear modulus is 1.35 MPa, the rolling friction coefficient between the pot and the pot is 0.25~0.55, the rolling friction coefficient between the pot and steel is 0.20~0.50, and the value of other necessary parameters of the discrete element simulation vary. To reduce the number of tests and obtain the determined parameter combination as soon as possible, the Plackett–Burman test design was carried out using Design-Expert software, and the parameters that significantly affect the test results were screened out, as shown in Table 3. Plackett Burman's experimental design is carried out for the eight uncertain parameters in the table, and the minimum and maximum values of the eight parameters are coded at −1 and +1, respectively.

Table 3. Test parameters of Plackett–Burman.

Simulation Parameters	Levels	
	−1	**+1**
The pot-steel restitution coefficient X_1	0.18	0.27
The pot-steel static friction X_2	0.73	0.85
The pot-steel rolling friction coefficient X_3	0.20	0.50
The pot-pot restitution coefficient X_4	0.29	0.37
The pot-pot static friction X_5	0.86	0.92
The pot-pot rolling friction coefficient X_6	0.25	0.55
Bond stiffness X_7/N·m^{-3}	0.7×10^6	1×10^6
Critical stress X_8/Pa	1.5×10^4	3×10^4
Bond radius X_9/mm	1.32	2.20

In this study, a central point was set (the median value of high and low levels was taken as the 0 levels), and 12 tests were conducted. The test results of each group of impact forces are obtained by EDEM software simulation, and the test design and results are shown in Table 4.

Table 4. Design and results of Plackett–Burman test.

No.	X_1	X_2	X_3	X_4	X_5	X_6	X_7	X_8	X_9	The Impact Force of the Collision between the Pot and the Steel Plate/N
1	1	1	−1	1	1	1	−1	−1	−1	11.00
2	1	1	1	−1	−1	−1	1	−1	1	14.38
3	1	−1	1	1	1	−1	−1	−1	1	15.13
4	1	−1	−1	−1	1	−1	1	1	−1	12.66
5	1	1	−1	−1	−1	1	−1	1	1	15.22
6	−1	−1	−1	1	−1	1	1	−1	1	10.05
7	−1	1	1	−1	1	1	1	−1	−1	15.08
8	−1	−1	1	−1	1	1	1	1	1	15.10
9	−1	−1	−1	−1	−1	−1	−1	−1	−1	8.65
10	−1	1	−1	1	1	−1	1	1	1	14.16
11	−1	1	1	1	−1	−1	−1	1	−1	8.84
12	1	−1	1	1	−1	1	1	1	−1	9.98

The analysis of the variance of the PB test using Design-Expert software yielded significant results for each parameter, as shown in Table 5. The pot-pot collision restitution coefficient X_4, bond radius X_9, and pot-to-steel static friction coefficient X_2 have significant effects on the collision impact force between the pot and the steel plate.

Table 5. Significance analysis of Plackett–Burman test parameters.

Term	Standardized Effects	Sum of Squares	Contrition	Significance Level
X_1	−1.15	4.00	5.39	4
X_2	1.84	10.10	13.62	3
X_3	−0.40	0.48	0.64	7
X_4	1.92	11.00	14.83	2
X_5	0.35	0.37	0.50	8
X_6	0.29	0.26	0.35	9
X_7	−0.44	0.58	0.78	6
X_8	1.11	3.71	5.00	5
X_9	3.80	43.43	58.55	1

4.2. Steepest Climbing Test

The three salient parameters obtained from the Plackett–Burman test were subjected to the steepest climb test, which can quickly approach the optimal parameter region. Each significant parameter was gradually increased in its value range according to the fixed step size. The other nonsignificant contact parameters were taken as the average values measured in physical tests: the restitution coefficient of collision between the pot and steel was 0.225, the rolling friction coefficient of the pot and steel was 0.35, the static friction coefficient of the pot and the pot was 0.89, the rolling friction coefficient of the pot and the pot was 0.4, and the bond stiffness was 0.85×10^6 N·m^3. The results are shown in Table 6, where the critical stress is 2.25×10^4 Pa, and the simulation test of the impact force of a 50-hole plug seedling pot falling onto the steel plate is carried out. With the gradual increase in the significant parameters, the relative error between the simulated and actual values decreases and then increases; a minor relative error is obtained under the corresponding parameter combination of test No. 3, which shows that the optimal parameter level ranges near test No. 3.

Table 6. Design and results of steepest climbing test.

No.	The Pot-Steel Static Friction X_2	The Pot-Pot Restitution Coefficient X_4	Bond Radius X_9/mm	The Impact Force of the Collision between the Pot and the Steel Plate/N	Relative Error/%
1	0.73	0.29	1.32	9.43	−21.05
2	0.754	0.306	1.496	10.44	−11.38
3	0.778	0.322	1.672	11.58	−1.70
4	0.802	0.338	1.848	12.67	7.56
5	0.826	0.354	2.024	13.69	16.21
6	0.85	0.37	2.20	15.04	27.67

4.3. Box–Behnken Test and Analysis of Significant Contact Parameters

Test parameter No. 3 in the steepest climb test was taken as the middle level (0), and test parameters No. 2 and No. 4 were taken as the high (+1) and low (−1) levels, respectively. The significant contact parameters and levels are shown in Table 7, and Design-Expert software was used to apply the Box–Behnken test. The values of other nonsignificant parameters are the same as the steepest climbing test. The Box–Behnken test design and results of significant contact parameters are shown in Table 8.

Table 7. Levels of significant contact parameters.

Levels	X_5	X_7/(N·m^{-3})	X_9/mm
+1	0.754	0.306	1.496
0	0.778	0.322	1.672
−1	0.802	0.338	1.848

The multiple regression analysis of the experimental results in Table 8 was performed using Design-Expert software to obtain a second-order regression model of stress with three significant parameters with the equation:

$$F = 13.51 - 1.15\,X_2 - 0.41\,X_4 + 1.18\,X_9 + 0.82\,X_2X_4 + 0.62\,X_2X_9 - 0.013\,X_4X_9 - 1.29\,{X_2}^2 + 0.18\,{X_4}^2 + 0.41\,{X_9}^2 \quad (7)$$

The fitted model has $p < 0.05$, the coefficient of determination $R^2 = 0.998$, the corrected coefficient of determination $R^2{}_{adj} = 0.8501$, both of which are close to 1, and the signal-to-noise ratio (Adeq precision) is 8.379, indicating that the stress regression model is significant and can predict the target; the misfit term $p = 0.389 > 0.05$, indicating that the equation fits well and has credibility. The results of the regression of the model are shown in Table 9, which shows that the bond radius X_9 has a significant effect on the collision impact between the pot and the steel plate; the quadratic terms X_2 and X_2^2 of the static friction coefficient between the pot and the steel have a significant effect on the collision impact between the pot and steel plate; the collision restitution coefficient between the pot X_4, the interaction terms X_2 X_4, X_2 X_9, X_4 X_9 and the quadratic terms X_4^2 and X_9^2 have no significant effects on the collision impact force between the pot and the steel plate.

Table 8. Box–Behnken experimental design and results of significant contact parameters.

No.	The Pot-Steel Static Friction X_2	The Pot-Pot Restitution Coefficient X_4	Bond Radius X_9/mm	The Impact Force of the Collision between the Pot and the Steel Plate/N
1	0	1	1	14.95
2	0	0	0	14.24
3	1	1	0	11.59
4	0	1	−1	13.24
5	1	0	−1	9.04
6	−1	1	0	11.56
7	−1	0	−1	13.25
8	0	−1	1	14.98
9	−1	−1	0	14.84
10	0	0	0	12.89
11	0	0	0	12.88
12	0	0	0	12.85
13	−1	0	1	14.98
14	0	0	0	14.67
15	1	−1	0	11.59
16	1	0	1	13.25
17	0	−1	−1	13.22

Table 9. Variation analysis of Box–Behnken design quadratic model.

Source of Variation	Mean Square	Degree of Freedom	Sum of Square	p Value
Model	34.71	9	3.86	0.0316 *
X_2	10.49	1	10.49	0.0105 *
X_4	1.35	1	1.35	0.2535
X_9	11.07	1	11.07	0.0092 **
X_2X_4	2.69	1	2.69	0.1229
X_2X_9	1.54	1	1.54	0.2264
X_4X_9	0.000625	1	0.000625	0.9794
X_2^2	7.00	1	7.00	0.0254 *
X_4^2	0.13	1	0.13	0.7073
X_9^2	0.72	1	0.72	0.3946
Residual	6.12	7	0.87	
Lack of fit	3.02	3	1.01	0.3890
Pure error	3.10	4	0.77	
Sum	40.83	16		

Note: ** indicates extremely significant ($p < 0.01$), * indicates significant ($0.01 < p < 0.05$).

4.4. Regression Model Interactive Response Analysis

A response surface analysis diagram and corresponding contour map of different factors were obtained using Design-Expert software, as shown in Figure 9. The response surface graph is a curved surface of the three-dimensional space formed by the response value to the static friction coefficient between the pot and steel, the collision restitution coefficient between the pot and the pot, and the bond radius of each test factor. From the response surface analysis graph, the impact of the interaction of various factors on the collision impact force between the pot and the steel plate can be clearly seen. If the curve is steeper, this factor significantly impacts the impact force between the pot and the steel plate, represented by the change in the response value. The contour map shows that the greater the curvature of the contour is, the more significant the interaction between the two parameters.

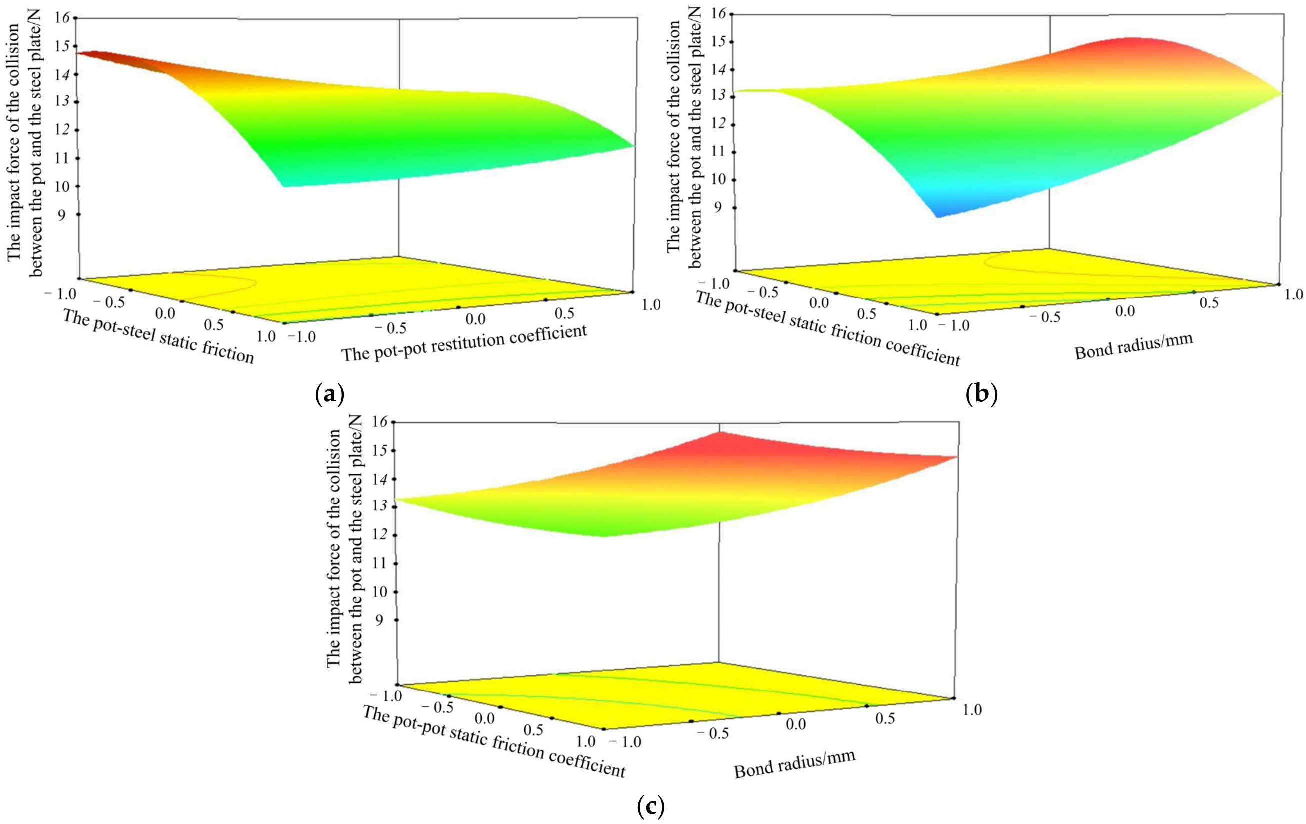

Figure 9. Interaction response surface plot. (**a**) The pot-steel static friction coefficient and the pot restitution coefficient; (**b**) The pot-steel static friction coefficient and the bond radius; (**c**) The pot restitution coefficient and bond radius.

As shown in Figure 9a, the static friction coefficient between the pot and steel and the impact restitution coefficient between the pot and the steel plate significantly impact the force between the pot and the steel plate. The curve slope changes significantly, indicating that the static friction coefficient between the pot and steel and the impact restitution coefficient between the pot and the steel plate has a significant impact on the impact force between the pot and the steel plate. The curvature of the contour line is large, which indicates that the interaction between the static friction coefficient between the pot and the steel and the collision restitution coefficient between the pot and the pot is significant. Figure 9b shows the impact of the pot and steel's static friction coefficient and bond radius on the impact force of the pot and the steel plate. The slope of the curved surface changes considerably, indicating that the static friction coefficient and bond radius of the pot and steel have a significant impact on the impact force of the pot and the steel plate. The curvature of the contour line is large, which indicates that the interaction of the pot and steel static friction coefficient and bond radius is significant. As shown in Figure 9c, the impact restitution coefficient between the pot and the pot and bond radius significantly impacts the impact force of the pot and the steel plate. The slope of the curved surface has a significant change, indicating that the bond stiffness and bond radius have a significant impact on the impact force of the pot and the steel plate. The curvature of the contour is slight, which indicates that the interaction between the collision restitution coefficient between the pot and the pot and the bond radius is not significant.

4.5. Verification and Determination of Optimal Parameter Combination for Simulation

Using the optimization module of Design-Expert software, the regression model Equation (7) was optimized with the target value of 11.78 N for the collision impact force of a 50-hole plug seedling pot falling on the steel plate at the height of 350 mm and a set of parameters similar to the physical test data were obtained: the static friction coefficient between the pot and the steel plate is 0.790, the collision restitution coefficient between the pot and the pot is 0.325, the bond radius of 1.542 mm, and the values of the remaining non-significant parameters are the same as those of the steepest climbing test. In order to check whether the optimal combination of parameters meets the simulation test results, the above parameters are input into EDEM software for simulation, the pot discrete element model is obtained, repeat the simulation tests are performed three times, and the simulation impact force is 11.76 N, 11.78 N, 11.77 N, respectively. The relative error between the simulation impact force average value of 11.77 N and the actual test impact force value is 0.084%, indicating that the model is reliable. It is feasible to use the above optimization tests to calibrate the discrete element simulation parameters.

5. Conclusions

(1) The collision restitution coefficients between the pot and the pot measured by high-speed camera ranged from 0.29 to 0.36, and between the pot and steel ranged from 0.18 to 0.27; the static friction coefficients between the pot and the pot measured by inclinometer ranged from 0.86 to 0.92, and between the pot and steel ranged from 0.73 to 0.85.

(2) The Plackett–Burman test was carried out based on the physical test results of contact parameters. The results of the variance analysis showed that the impact restitution coefficient X_4, the bond radius X_9, and the impact restitution coefficient X_1 between the pot and the pot significantly impacted the impact force between the pot and the steel plate.

(3) Taking the 11.78 N test value of the impact force between the pot and the steel plate measured by the flexible film network tactile pressure sensor as the target, the optimal solution of the significant parameters is obtained: the static friction coefficient between the pot and the steel plate is 0.790, the impact restitution coefficient between the pot and the pot is 0.325, and the bond radius is 1.542 mm.

(4) Experimental verification of the optimization results shows that the average impact force of the simulated collision between the pot and the steel plate under the optimized parameter combination is 11.77 N. The relative error with the actual value is 0.084%, which indicates that the model is reliable. Applying each of the above optimization tests to calibrate the discrete element simulation parameters is feasible.

Author Contributions: Conceptualization, X.L.; methodology, J.C. and F.Z.; software, J.C. and H.B.; data curation, J.C. and Y.Z.; formal analysis, writing—original draft preparation, writing review and editing, J.C. All authors have read and agreed to the published version of the manuscript.

Funding: This project was funded by National Natural Science Foundation of China (NSFC) (32160423) and the Natural Science Foundation of the Inner Mongolia Autonomous Region of China (2020MS05055).

Institutional Review Board Statement: Not applicable.

Informed Consent Statement: Not applicable.

Data Availability Statement: Not applicable.

Acknowledgments: The authors gratefully acknowledge the financial support provided by the National Natural Science Foundation of China (NSFC) (32160423) and the Natural Science Foundation of the Inner Mongolia Autonomous Region of China (2020MS05055). We also appreciate the work of the editors and the reviewers of the paper.

Conflicts of Interest: The authors declare no conflict of interest.

References

1. Hu, Y.Y. Research on Countermeasures for the Development of Sunflower Production in Heilongjiang Province. Master's Thesis, Chinese Academy of Agricultural Sciences, Beijing, China, 2014.
2. Zhou, C.Y.; Bai, G.S.; Du, S.N. Effects of spring wheat sunflower replanting on soil salinity and farmland productivity in Hetao area. *J. China Agric. Univ.* **2017**, *22*, 1–10.
3. Zhou, Z.W. Design and Research of Planting Depth Control System of Hanging Cup Transplanting Machine. Master's Thesis, Inner Mongolia Agricultural University, Hohhot, China, 2021.
4. Jorg, O.J.; Sportelli, M.; Fontanelli, M.; Frasconi, C.; Fantoni, G. Design, Development and Testing of Feeding Grippers for Vegetable Plug Transplanters. *AgriEngineering* **2021**, *3*, 669–680. [CrossRef]
5. Sivakumar, S.; Durairaj, C.D. Development of a gravity fed automatic vegetable transplanter with walking beam mechanism. *Trends Biosci.* **2014**, *7*, 407–410.
6. Hu, S.Y.; Hu, M.J.; WANG, J. Research Progress on Mechanized Transplanting of Pepper Hole Seedlings. *Chin. J. Agric. Mech.* **2021**, *42*, 24–31. [CrossRef]
7. Ma, Y.F.; Wang, W.B.; Feng, J.A.; Shen, T.H.; Guo, Z.Y. Experimental study on clamping compression characteristics of seedling bowl of transplanted tomato cave tray. *Chin. J. Agric. Mech.* **2020**, *41*, 64.
8. Zeng, F.D.; Li, X.Y.; Li, X.; Su, Q.; Zhang, Y.Z. Experiment and analysis of high-speed photographic techniques for throwing motion of seedlings. *J. China Agric. Univ.* **2021**, *26*, 168–176.
9. Hu, J.P.; Liu, Y.T.; Liu, W.; Zhang, S.W.; Han, L.H.; Zeng, T.Y. Experimental study on the top clamping combined seedling taking device of vegetable automatic transplanting machine. *Trans. Chin. Soc. Agric. Machinery* **2022**, *53*, 110–117.
10. Fang, H.M.; Ji, C.Y.; Farman, A.C.; Guo, J.; Zhang, Q.Y.; Chaudhry, A. Analysis of soil movement behavior in rotary tillage process based on discrete element method. *Trans. Chin. Soc. Agric. Mach.* **2016**, *47*, 22–28.
11. Milkevych, V.; Munkholm, L.J.; Chen, Y.; Nyord, T. Modelling approach for soil displacement in tillage using discrete element method. *Soil Tillage Res.* **2018**, *183*, 60–71. [CrossRef]
12. Murray, S.; Chen, Y. Discrete element modeling of soil displacement resulting from hoe openers. *Trans. ASABE* **2019**, *62*, 253–262. [CrossRef]
13. Zeng, Z.W.; Ma, X.; Cao, X.L.; LI, Z.H.; Wang, X.C. Application Status and Prospect of Discrete Element Method in Agricultural Engineering Research. *Trans. Chin. Soc. Agric. Mach.* **2021**, *52*, 1–20.
14. Horabik, J.; Parafiniuk, P.; Molenda, M. Experiments and discrete element method simulations of distribution of static load of grain bedding at bottom of shallow model silo. *Biosyst. Eng.* **2016**, *149*, 60–71. [CrossRef]
15. Tamás, K. The role of bond and damping in the discrete element model of soil-sweep interaction. *Biosyst. Eng.* **2018**, *169*, 57–70. [CrossRef]
16. Wang, L.J.; Liu, T.H.; Feng, X.; Gao, Y.P.; Wang, B. Research progress on particle collision recovery coefficients in agriculture and food. *Trans. Chin. Soc. Agric. Eng.* **2021**, *37*, 313–322.
17. Liu, C.; Chen, X.X.; Zhang, W.; Wang, S. Study on the calibration process of parallel bonding mesoparameters in PFC numerical simulation. *Value Eng.* **2017**, *36*, 204–207.
18. Wang, Y.X.; Liang, Z.J.; Zhang, D.X.; Cui, T.; Shi, S.; Li, K.H.; Yang, L. Discrete-based calibration of interspecific contact parameters in maize seed granule models. *Trans. Chin. Soc. Agric. Eng.* **2016**, *32*, 36–42.
19. Zhang, R.F.J.W.; Zhou, J.L.; Qi, B.; Liu, H.; Xia, Q.Q. Calibration of discrete element model parameters of rice seeds with different filled particle radii. *Trans. Chin. Soc. Agric. Mach.* **2020**, *51*, 227–235.
20. Zhang, T.; Liu, F.; Zhao, M.Q.; LIiu, Y.Q.; Li, F.L.; Ma, Y.; Zhou, Q.; Zhao, P. Determination of physical parameters of contact between soybean seeds and seeders and discrete element simulation calibration. *J. China Agric. Univ.* **2017**, *22*, 86–92.
21. Shi, R.J.; Dai, F.; Zhao, W.Y.; Zhang, F.W.; Shi, L.R.; Guo, J.H. Establishment of discrete element flexible model of flax stem and experimental verification of contact parameters. *Trans. Chin. Soc. Agric. Mach.* **2022**, *53*, 146–155.
22. Gao, G.; Wang, K.; Sun, X. Verification for EDEM simulation of process of jacking tray-seedling by steel needle in grafting machine and parameter optimization. *Trans. Chin. Soc. Agric. Eng.* **2017**, *33*, 29–35.
23. Han, B.; Shen, D.; Guo, C.; Liu, Q.; Wang, X.; Song, C. Design and experiment of adjustable end-effector of cabbage seedlings. *Trans. Chin. Soc. Agric. Mach.* **2019**, *50*, 111–120.
24. Tian, Z.; Ma, W.; Yang, Q.; Yao, S.; Guo, X.; Duan, F.J.A. Design and Experiment of Gripper for Greenhouse Plug Seedling Transplanting Based on EDM. *Agronomy* **2022**, *12*, 1487. [CrossRef]
25. Liu, W.Z.; He, J.; Li, H.W.; Li, X.Q.; Zheng, K.; Wei, Z.C. Discrete element-based micropotato simulation parameter calibration. *Trans. Chin. Soc. Agric. Mach.* **2018**, *49*, 125–135.
26. Dai, Z.; Wu, M.; Fang, Z.; Qu, Y. Calibration and Verification Test of Lily Bulb Simulation Parameters Based on Discrete Element Method. *Applied Sciences* **2021**, *11*, 10749. [CrossRef]
27. Sandeep, C.S.; Luo, L.; Senetakis, K. Effect of grain size and surface roughness on the normal coefficient of restitution of single grains. *Materials* **2020**, *13*, 814. [CrossRef]
28. Ma, Y.H.; Song, C.D.; Xuan, C.Z.; Wang, H.Y.; Yang, S.; Wu, P. Discrete-element model parameter calibration for alfalfa straw compression simulation. *Trans. Chin. Soc. Agric. Eng.* **2020**, *36*, 22–30.
29. Sun, X.; Li, B.; Liu, Y.; Gao, X. Parameter measurement of edible sunflower exudates and calibration of discrete element simulation parameters. *Processes* **2022**, *10*, 185. [CrossRef]

30. Zeng, F.; Li, X.; Bai, H.; Cui, J.; Liu, X.; Zhang, Y. Experimental Study on Pot Damage and Contact Stress Distribution Characteristics of Oil Sunflower Plug Seedlings. *Appl. Sci.* **2022**, *12*, 10889. [CrossRef]
31. Bai, H.; Li, X.; Zeng, F.; Cui, J.; Zhang, Y. Study on the Impact Damage Characteristics of Transplanting Seedlings Based on Pressure Distribution Measurement System. *Horticulturae* **2022**, *8*, 1080. [CrossRef]
32. Han, C.J.; XU, Y.; Yu, J.; Zhang, J.; Yuan, P.P. Optimization of the parameters of the cave generator of semi-automatic compression substrate type watermelon bowl seedling transplanting machine. *Trans. Chin. Soc. Agric. Eng.* **2019**, *35*, 48–56.
33. Tong, J.H.; Shi, H.F.; Wu, C.Y.; Ding, Y.H.; Zhao, X.; Wang, R.Y. Simulation and test of seedling pot substrate grasping of acupuncture tray transplanting finger shovel end effector. *Trans. Chin. Soc. Agric. Mach.* **2019**, *50*, 107–116.
34. Wang, Y.; Chen, J.N.; Wu, J.W.; Zhao, Y. Mechanical properties test of broccoli bowl seedlings for mechanized cultivation. *Trans. Chin. Soc. Agric. Eng.* **2014**, *30*, 1–10.